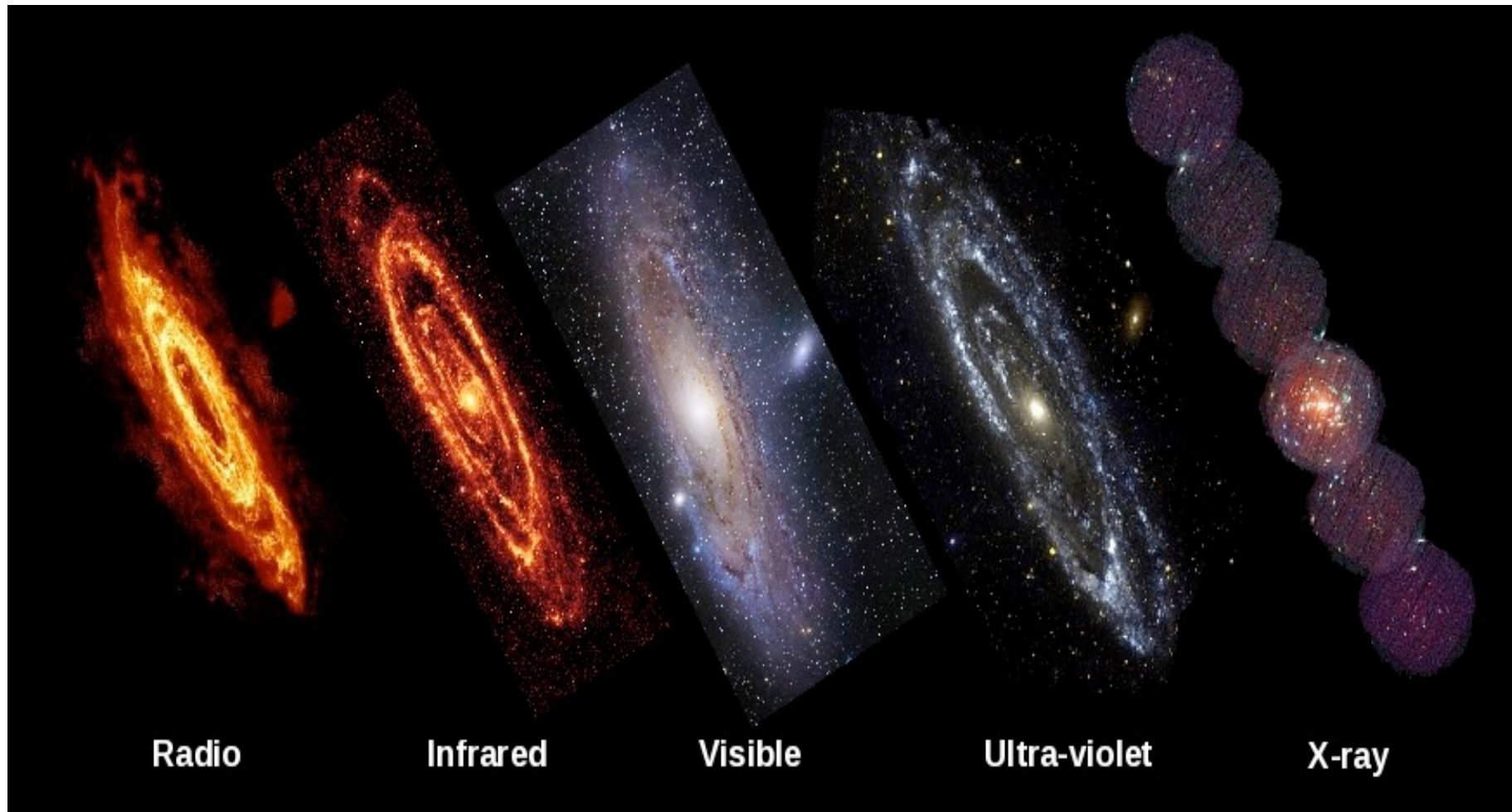


Star Formation Rates in Galaxies



Radio

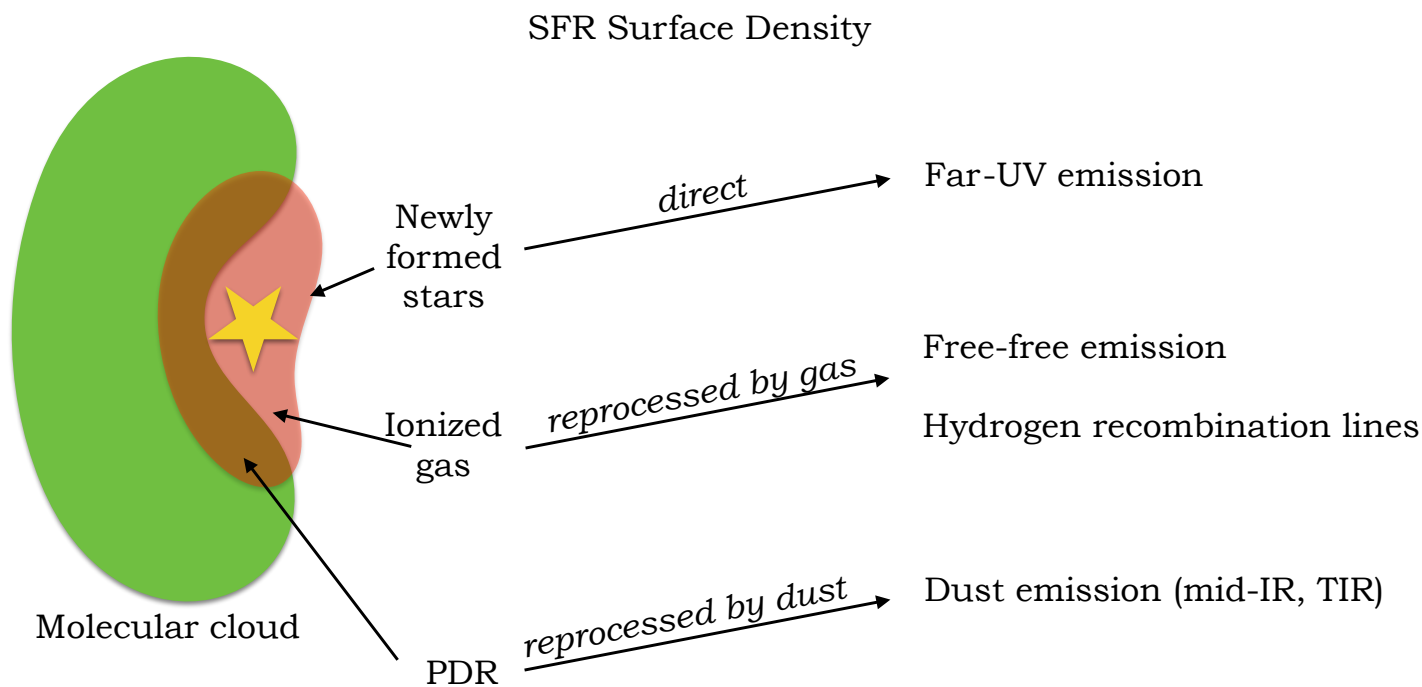
Infrared

Visible

Ultra-violet

X-ray

Making the measurements...



Measuring Star Formation Rates #1: Linear relations between luminosity and SFR.

(NOTE Below are out of date)

- L_{IR}
$$\frac{\text{SFR}}{1 M_{\odot} \text{ yr}^{-1}} = \frac{L_{\text{FIR}}}{2.2 \times 10^{43} \text{ ergs s}^{-1}} = \frac{L_{\text{FIR}}}{5.8 \times 10^9 L_{\odot}}.$$
- L_{UV}
$$\text{SFR}(M_{\odot} \text{ yr}^{-1}) = 1.4 \times 10^{-28} L_{\nu}(\text{UV}) (\text{erg s}^{-1} \text{ Hz}^{-1}).$$
- $L_{\text{H}\alpha}$
$$\text{SFR}(M_{\odot} \text{ yr}^{-1}) = 7.9 \times 10^{-42} L(\text{H}\alpha) (\text{erg s}^{-1})$$

Kennicutt 1998 ARA&A 36: Assumes a Salpeter IMF, with mass limits from 0.1 to 100 Msun and Solar metal abundances. SFR is assumed to be constant over the past 10 Myr (for UV) and 100 Myr (for Halpha). $L(\text{UV})$ must be corrected for dust extinction.

Recall : Initial Mass Function

$$\xi(M)dM = \xi_0(M/M_\odot)^{-\alpha} \frac{dM}{M_\odot}$$

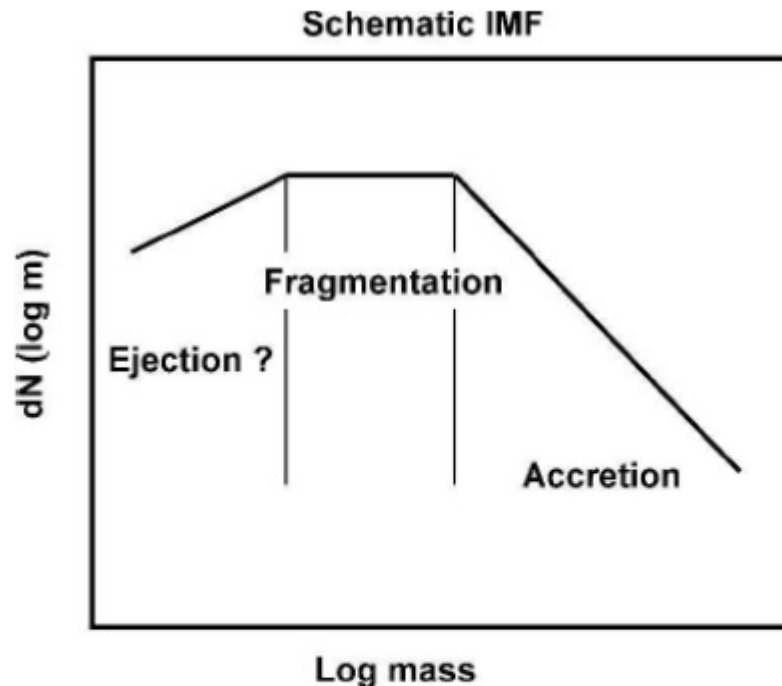
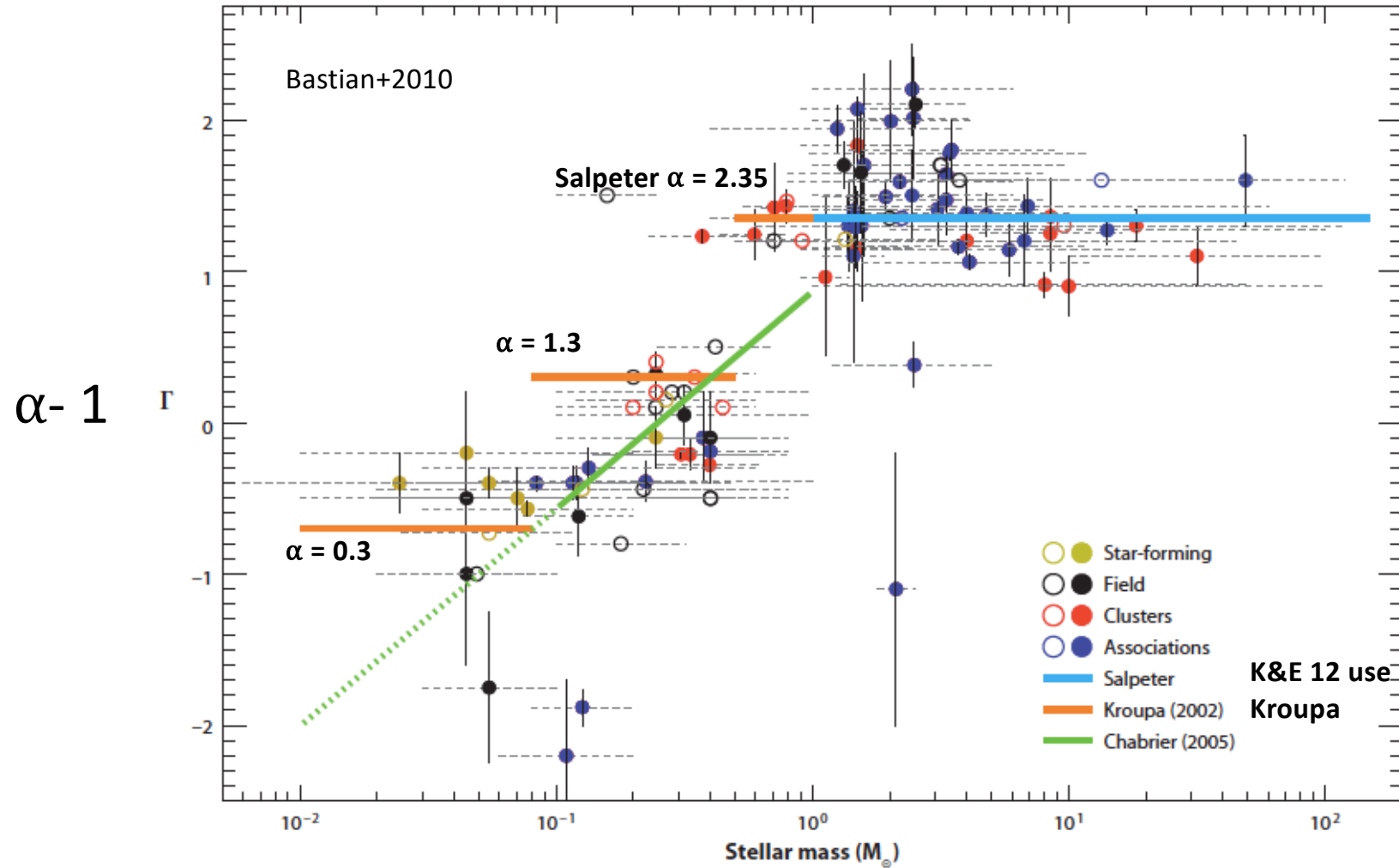


Fig. 11.— A schematic IMF showing the regions that are expected to be due to the individual processes. The peak of the IMF and the characteristic stellar mass are believed to be due to gravitational fragmentation, while lower mass stars are best understood as being due to fragmentation plus ejection or truncated accretion while higher-mass stars are understood as being due to accretion.



K98 UPDATED !!

$$\log \dot{M}_*(\text{M}_\odot \text{ year}^{-1}) = \log L_x - \log C_x.$$

Kennicutt & Evans 2012
eqn 12. Kroupa IMF

Table 1 Star-formation-rate calibrations

Band	Age range (Myr) ^a	L_x units	$\log C_x$ ^b	$\dot{M}_*/\dot{M}_*(\text{K98})$ ^c	Reference(s)
FUV	0-10-100	ergs s ⁻¹ (νL_ν)	43.35	0.63	Hao et al. (2011), Murphy et al. (2011)
NUV	0-10-200	ergs s ⁻¹ (νL_ν)	43.17	0.64	Hao et al. (2011), Murphy et al. (2011)
H α	0-3-10	ergs s ⁻¹	41.27	0.68	Hao et al. (2011), Murphy et al. (2011)
TIR	0-5-100 ^d	ergs s ⁻¹ (3-1100 μm)	43.41	0.86	Hao et al. (2011), Murphy et al. (2011)
24 μm	0-5-100 ^d	ergs s ⁻¹ (νL_ν)	42.69		Rieke et al. (2009)
70 μm	0-5-100 ^d	ergs s ⁻¹ (νL_ν)	43.23		Calzetti et al. (2010b)
1.4 GHz	0-100	ergs s ⁻¹ Hz ⁻¹	28.20		Murphy et al. (2011)
2-10 keV	0-100	ergs s ⁻¹	39.77	0.86	Ranalli et al. (2003)

^aSecond number gives mean age of stellar population contributing to emission; third number gives age below which 90% of emission is contributed.

^bConversion factor between SFR and the relevant luminosity, as defined by Equation 12 in Section 3.8.

^cRatio of star-formation rate (SFR) derived using the new calibration to that derived using the relations in Kennicutt (1998a). The lower SFRs now mainly result from the different initial mass function and from updated stellar population models.

^dNumbers are sensitive to star-formation history; those given are for continuous star formation over 0-100 Myr. For more quiescent regions (e.g., disks of normal galaxies), the maximum age will be considerably longer.

Abbreviations: FUV, far ultraviolet; NUV, near ultraviolet; TIR, total infrared.

****Note: Assumes solar metallicity

Table 2 Multiwavelength dust corrections for normal galaxies

Composite tracer	Reference
$L(\text{FUV})_{\text{corr}} = L(\text{FUV})_{\text{obs}} + 0.46 L(\text{TIR})$	Hao et al. (2011)
$L(\text{FUV})_{\text{corr}} = L(\text{FUV})_{\text{obs}} + 3.89 L(25 \mu\text{m})$	Hao et al. (2011)
$L(\text{FUV})_{\text{corr}} = L(\text{FUV})_{\text{obs}} + 7.2 \times 10^{14} L(1.4 \text{ GHz})^{\text{a}}$	Hao et al. (2011)
$L(\text{NUV})_{\text{corr}} = L(\text{NUV})_{\text{obs}} + 0.27 L(\text{TIR})$	Hao et al. (2011)
$L(\text{NUV})_{\text{corr}} = L(\text{NUV})_{\text{obs}} + 2.26 L(25 \mu\text{m})$	Hao et al. (2011)
$L(\text{NUV})_{\text{corr}} = L(\text{NUV})_{\text{obs}} + 4.2 \times 10^{14} L(1.4 \text{ GHz})^{\text{a}}$	Hao et al. (2011)
$L(\text{H}\alpha)_{\text{corr}} = L(\text{H}\alpha)_{\text{obs}} + 0.0024 L(\text{TIR})$	Kennicutt et al. (2009)
$L(\text{H}\alpha)_{\text{corr}} = L(\text{H}\alpha)_{\text{obs}} + 0.020 L(25 \mu\text{m})$	Kennicutt et al. (2009)
$L(\text{H}\alpha)_{\text{corr}} = L(\text{H}\alpha)_{\text{obs}} + 0.011 L(8 \mu\text{m})$	Kennicutt et al. (2009)
$L(\text{H}\alpha)_{\text{corr}} = L(\text{H}\alpha)_{\text{obs}} + 0.39 \times 10^{13} L(1.4 \text{ GHz})^{\text{a}}$	Kennicutt et al. (2009)

^aRadio luminosity in units of ergs s⁻¹ Hz⁻¹.

Abbreviations: FUV, far ultraviolet; NUV, near ultraviolet; TIR, total infrared.

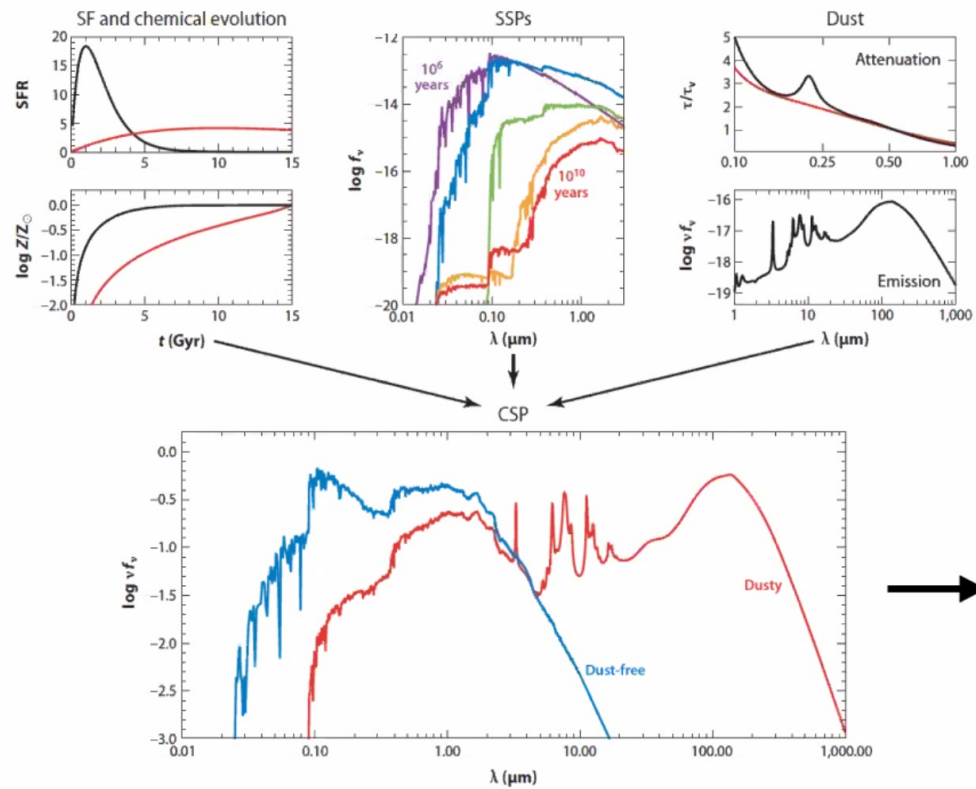
Lab 8 : part A – SFR of WLM



Irregular Dwarf Galaxy
Located at the edge of the
Local Group

Measuring Star Formation Rates #2 : SED Fitting

SPS Models: Tools for Interpreting Integrated Light



Conroy 2013

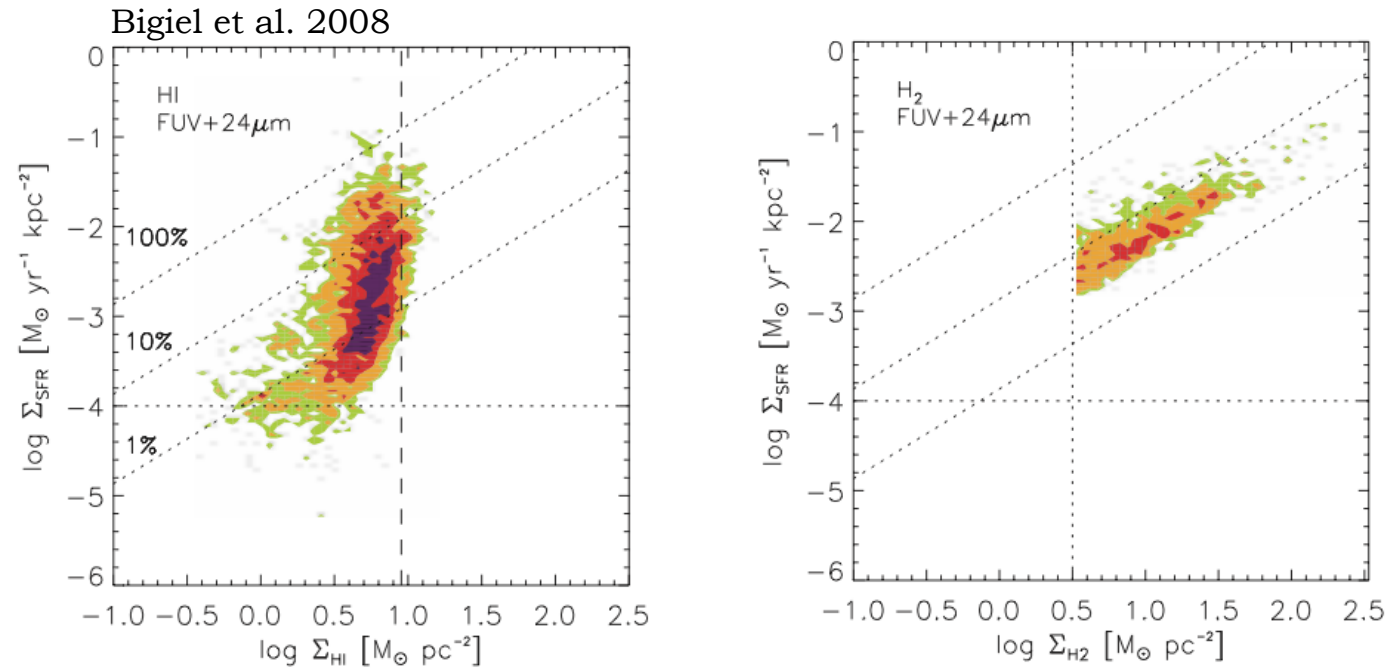
Fit to
observed
SEDs to infer
galaxy
properties

Measuring Star
Formation Rates #3 :
Gas Density

The Roles of HI and H₂

Kiloparsec scale

On kpc scales, SFR correlates best with H₂.



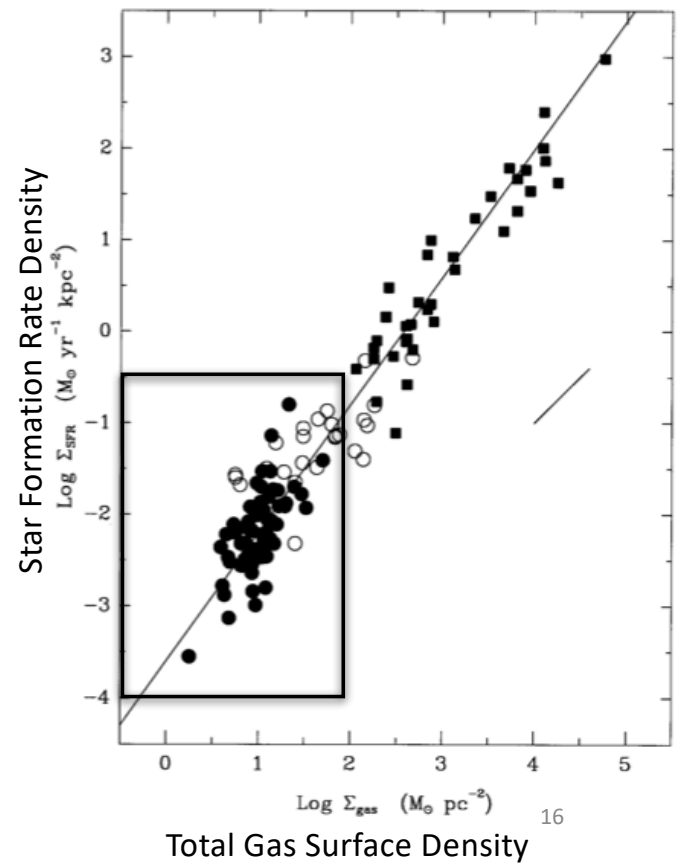
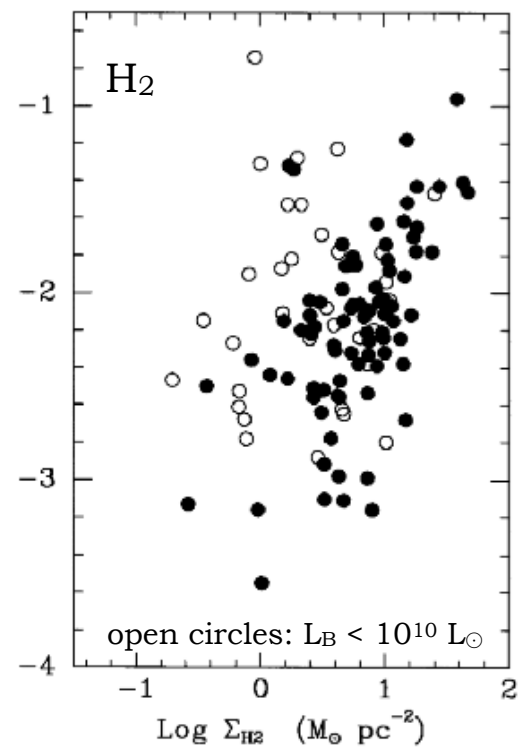
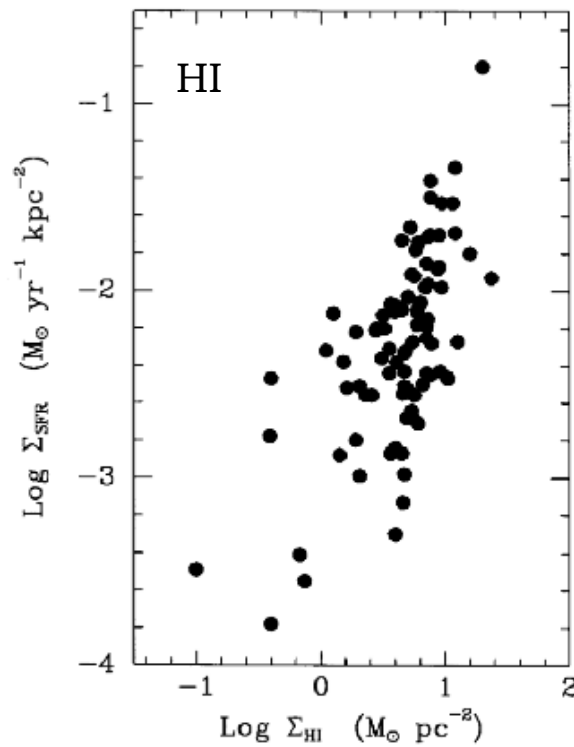
Rownd & Young 1999, Wong & Blitz 2002, Heyer et al. 2004,
Kennicutt et al. 2007, Bigiel et al. 2008, Leroy et al. 2008, others

Slides: Karin Sandstrom

On Galaxy Scales SFR best correlated with total gas - better than HI or H₂ alone.

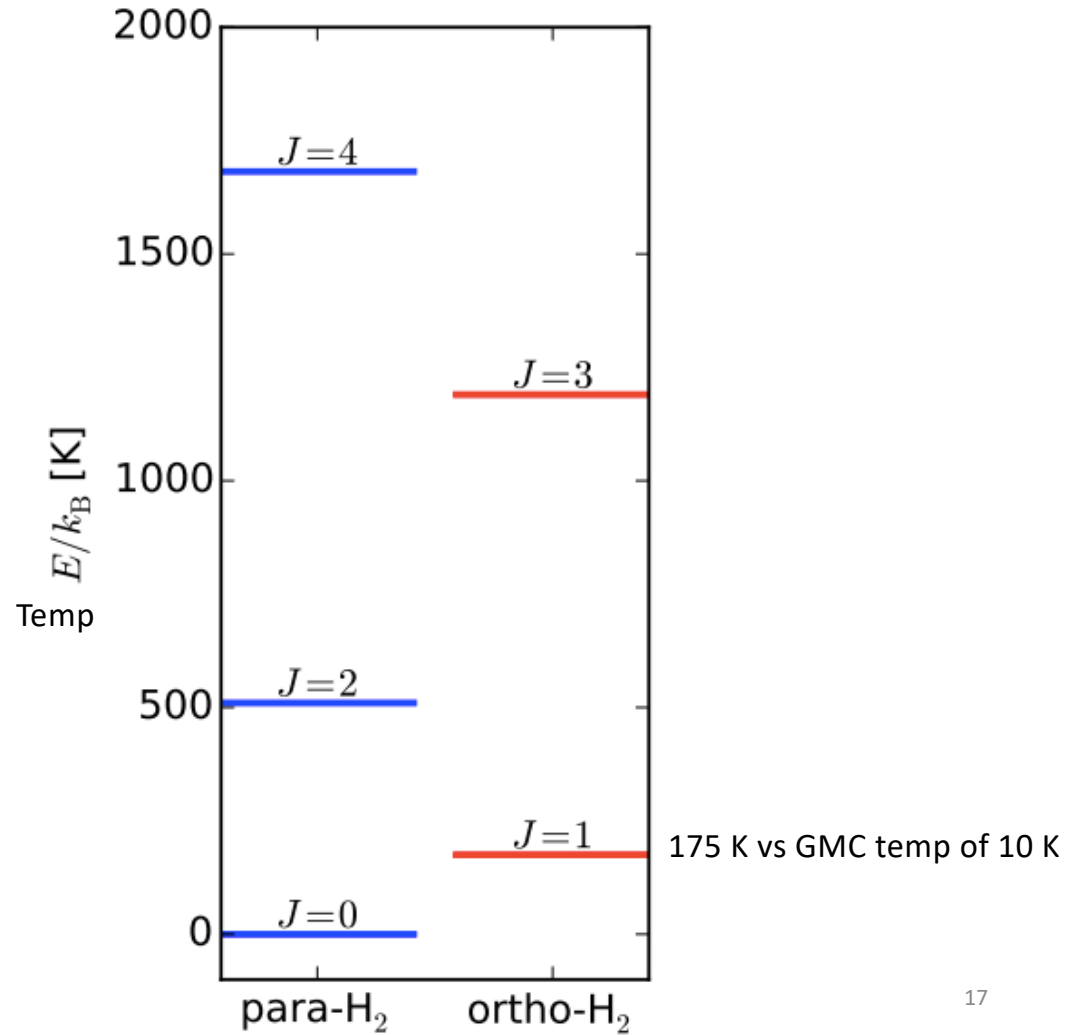
Scatter not explained by observational uncertainties.

Kennicutt 1998



H₂

Level diagram for the rotational levels of para- and ortho-H₂, showing the energy of each level.



Instead, folks infer H₂ using measurements of CO

$$N(\text{H}_2) = \underset{\text{Column density of H}_2}{X(\text{CO})} \underset{\text{Conversion factor}}{I(\text{CO})} \underset{-}{\text{Intensity of CO emission}}$$

$$X(\text{CO}) = 2.8 \times 10^{20} \text{ cm}^{-2} (\text{K km s}^{-1})^{-1} \quad \text{Kennicutt 1998b}$$

$$X(\text{CO}) = 2.0 \times 10^{20} \text{ cm}^{-2} (\text{K km s}^{-1})^{-1} \quad \begin{array}{l} \text{Pineda + 2010b} \\ \text{MW Value} \end{array}$$

Why this works ...

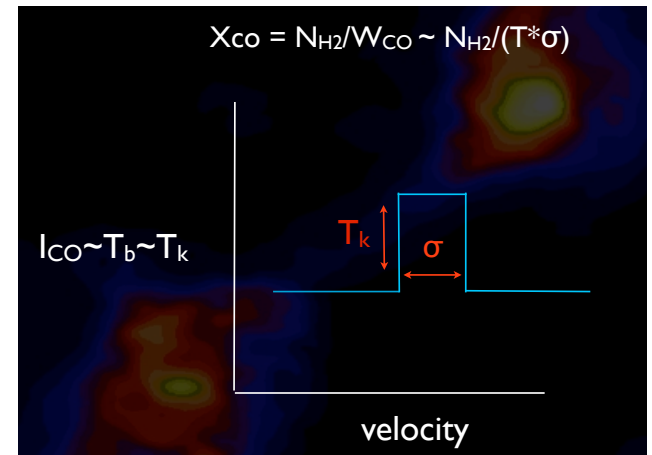
$$M(r) \propto \sigma^2 R \xrightarrow{\text{Virial Theorem}} M_{vir} \propto \sigma^4$$

$$\sigma = C R^{0.5} \quad \text{Larson 1981}$$

$$L_{CO} = \sqrt{2\pi^3} T_B \sigma R^2 \xrightarrow{\text{Surface brightness x area}} L_{CO} \propto T_B \sigma^5$$

Most of the mass is dominated by H₂

$$M_{vir} \approx M_{mol} \approx 200 \left(\frac{C^{1.5} L_{CO}}{T_B} \right)^{0.8}$$



Brightness temperature T_b is the temperature of a blackbody that would have the same brightness at the given frequency

C indicates the fraction of the cloud in the H₂ phase

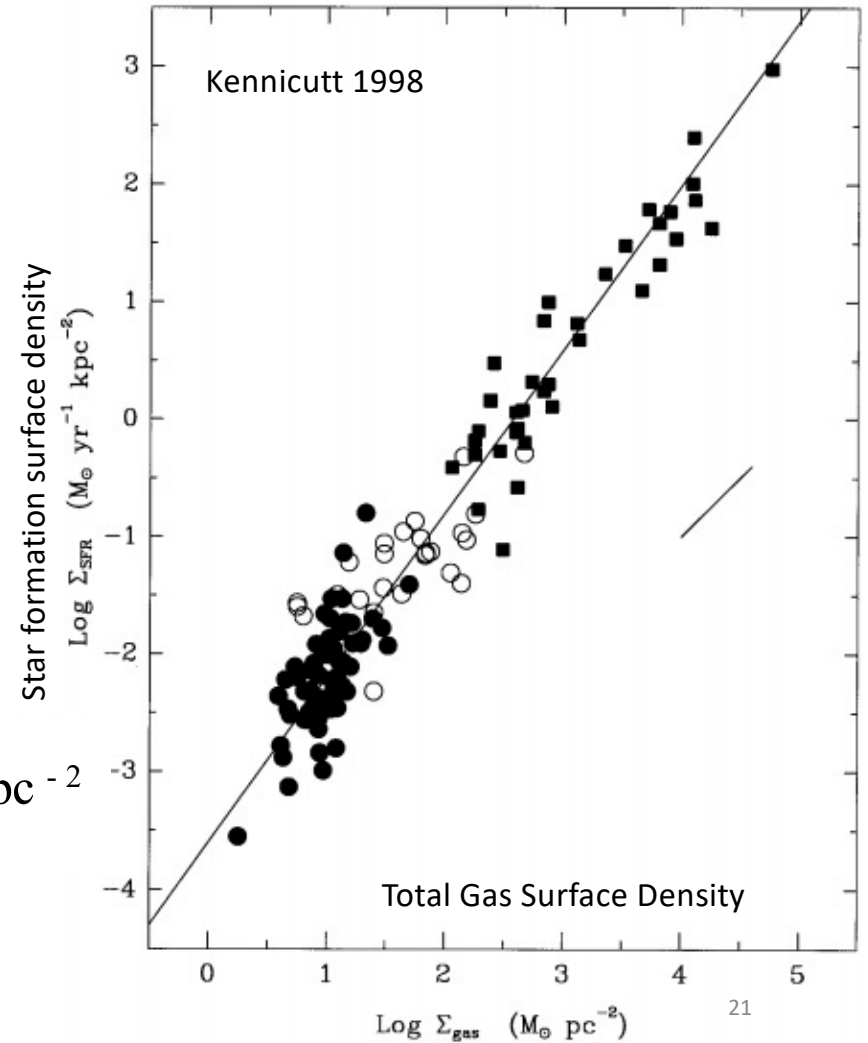
Bolatto+2013 Review

SFRs: Kennicutt-Schmidt Relation

$$\Sigma_{\text{SFR}} \propto \Sigma_{\text{gas}}^{1.4}$$

Higher surface densities represent more dense gas, yields higher SFR

$$\Sigma_{\text{SFR}} = 2.510^{-4} \left(\frac{\Sigma_{\text{gas}}}{1 M_{\odot} \text{pc}^{-2}} \right)^{1.4} M_{\odot} \text{yr}^{-1} \text{kpc}^{-2}$$



Understanding the Kennicutt – Schmidt relation

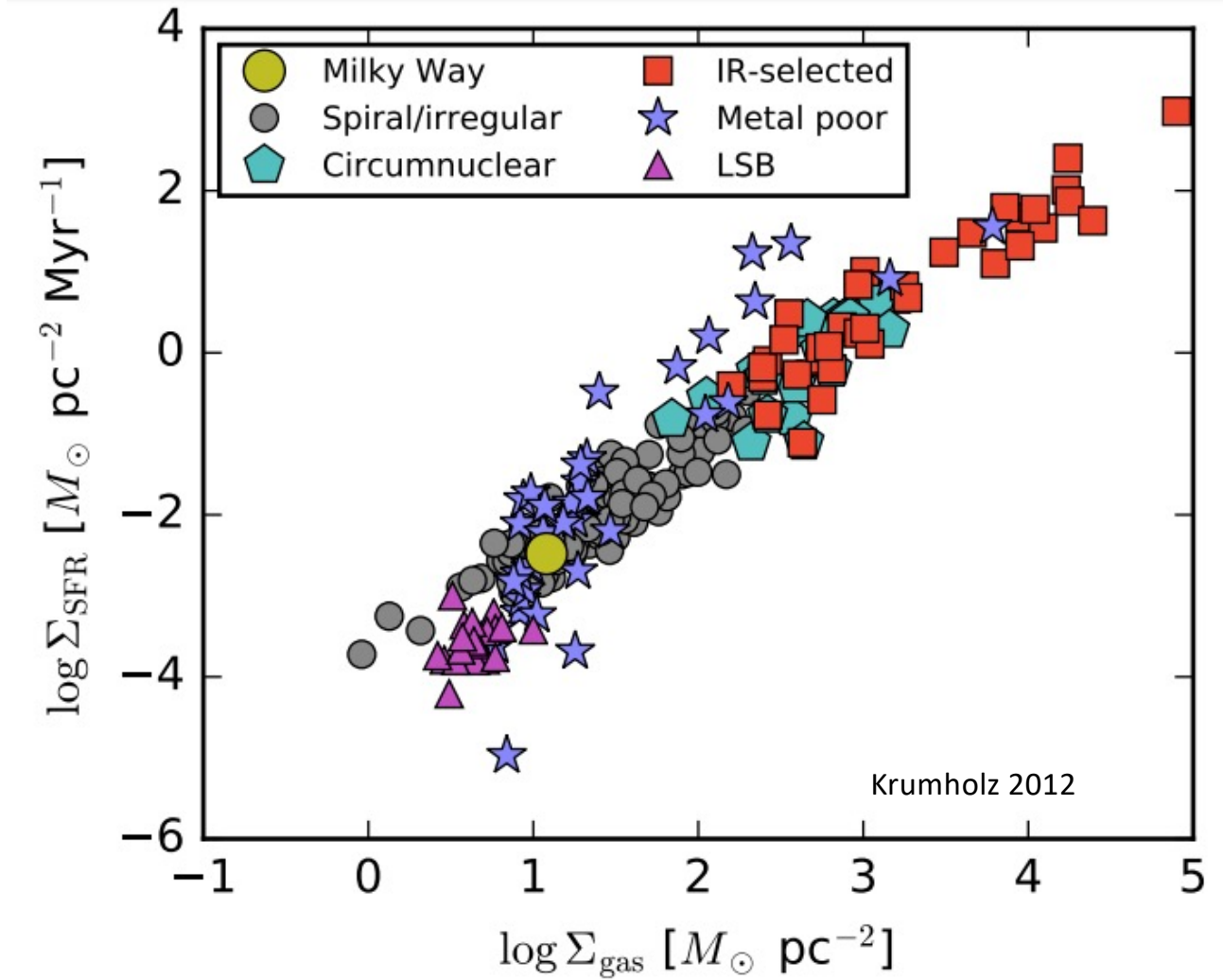
$$\text{SFR} \propto \rho_{\text{gas}} / \tau_{\text{ff}} \propto \rho_{\text{gas}}^{1.5}$$

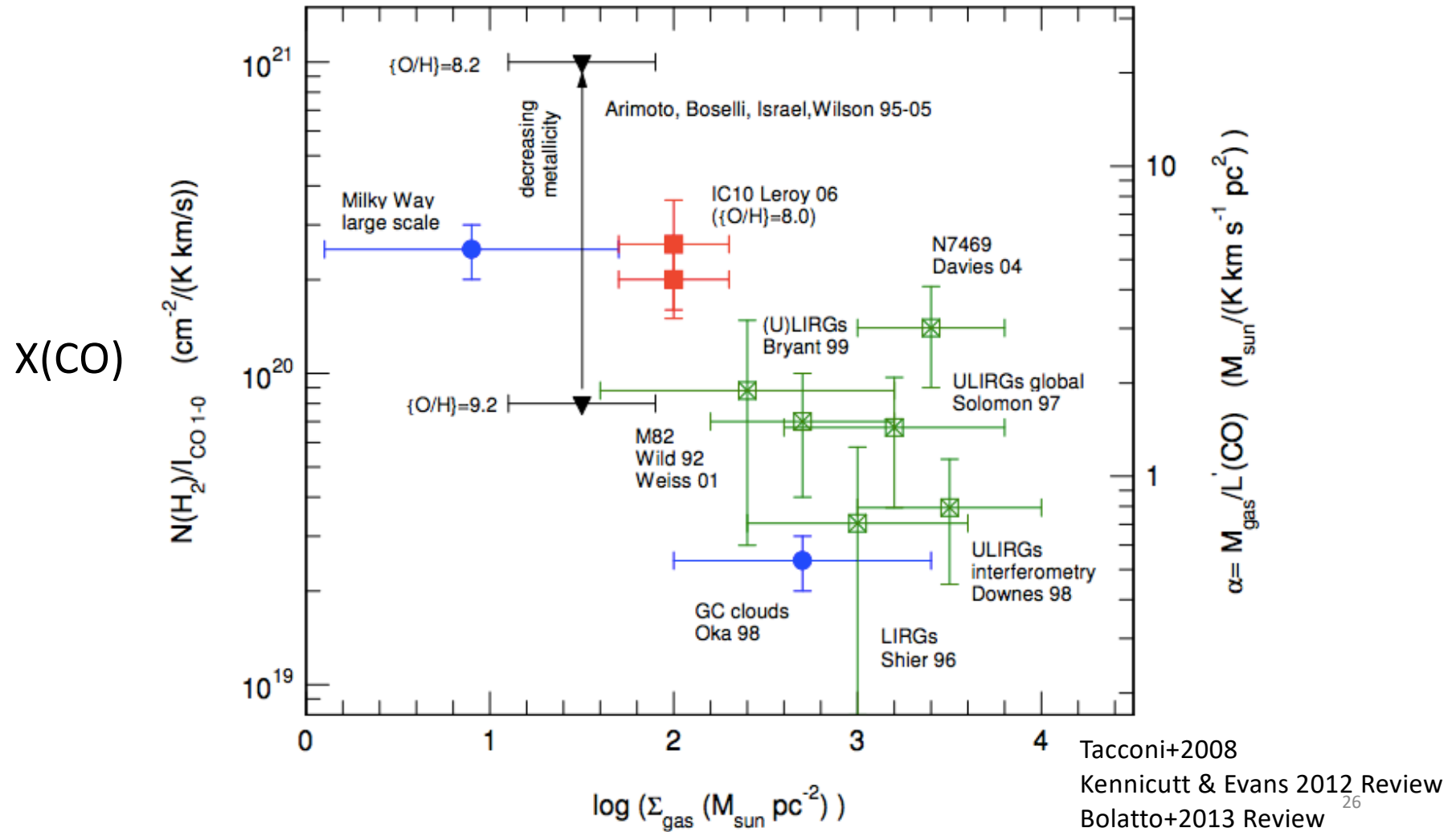
where $\tau_{\text{ff}} = (3\pi/(32 G \rho_{\text{gas}}))^{0.5}$ Cloud free-fall time,

Kennicutt-Schmidt

$$\Sigma_{\text{SFR}} \propto \Sigma_{\text{gas}}^{1.4}$$

LSB = low surface brightness galaxy

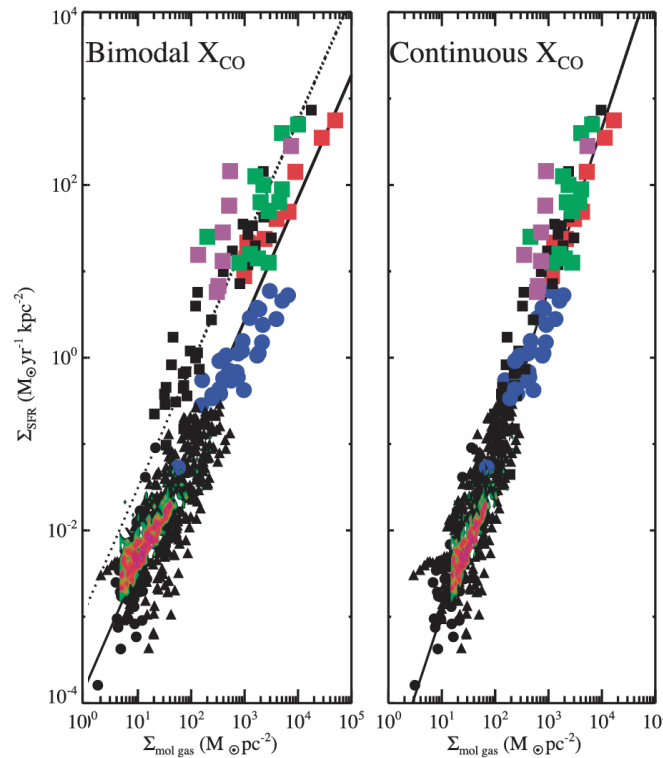




Kennicutt-Schmidt roughly holds at high z

Depending on the assumption of X_{CO} - 2 parallel sequences or one steeper sequence.

Narayanan + 2012 MNRAS 421



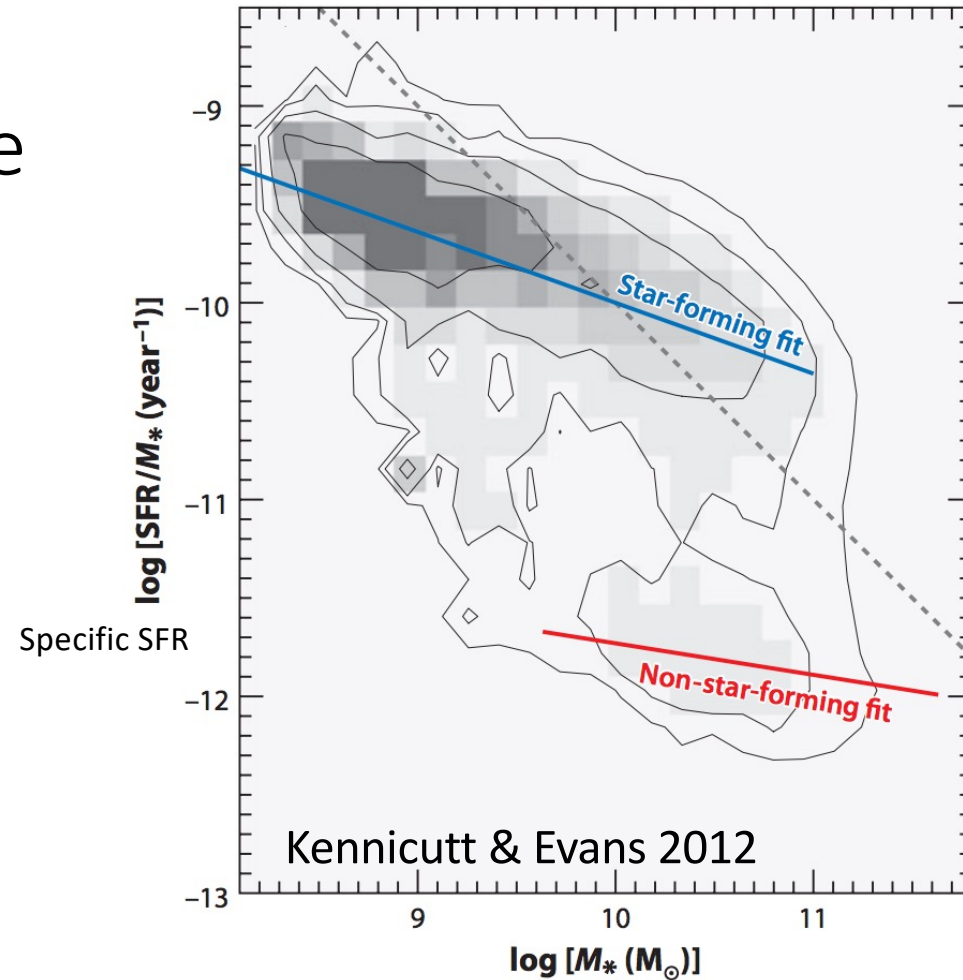
Circles and triangles are local discs or high-z star forming galaxies, and squares are inferred mergers (local ULIRGs or high-z SMGs).

Right: The power-law index in the relation is approximately 2

Star Formation Main Sequence

There is a tight relation between star formation rate and galaxy stellar mass

Brinchmann et al. 2004;
Noeske et al. 2007;
Elbaz et al. 2007,
Whitaker+2015



Lab 8 Part B: SF Main Sequence Evolution

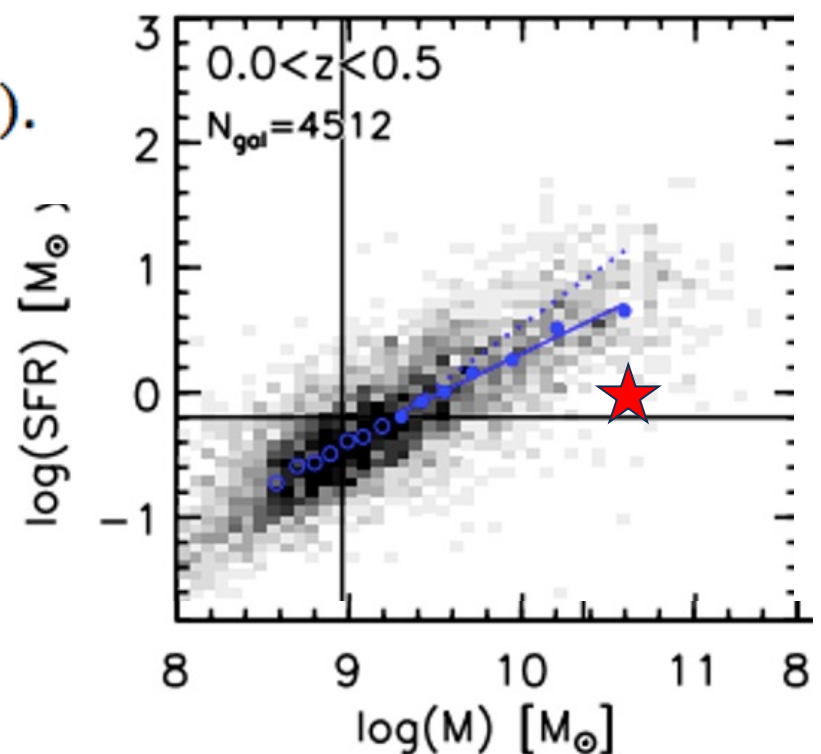
Whitaker+2012

$$\log(\text{SFR}) = \alpha(z)(\log M_{\star} - 10.5) + \beta(z).$$

$$\alpha(z) = 0.70 - 0.13z$$

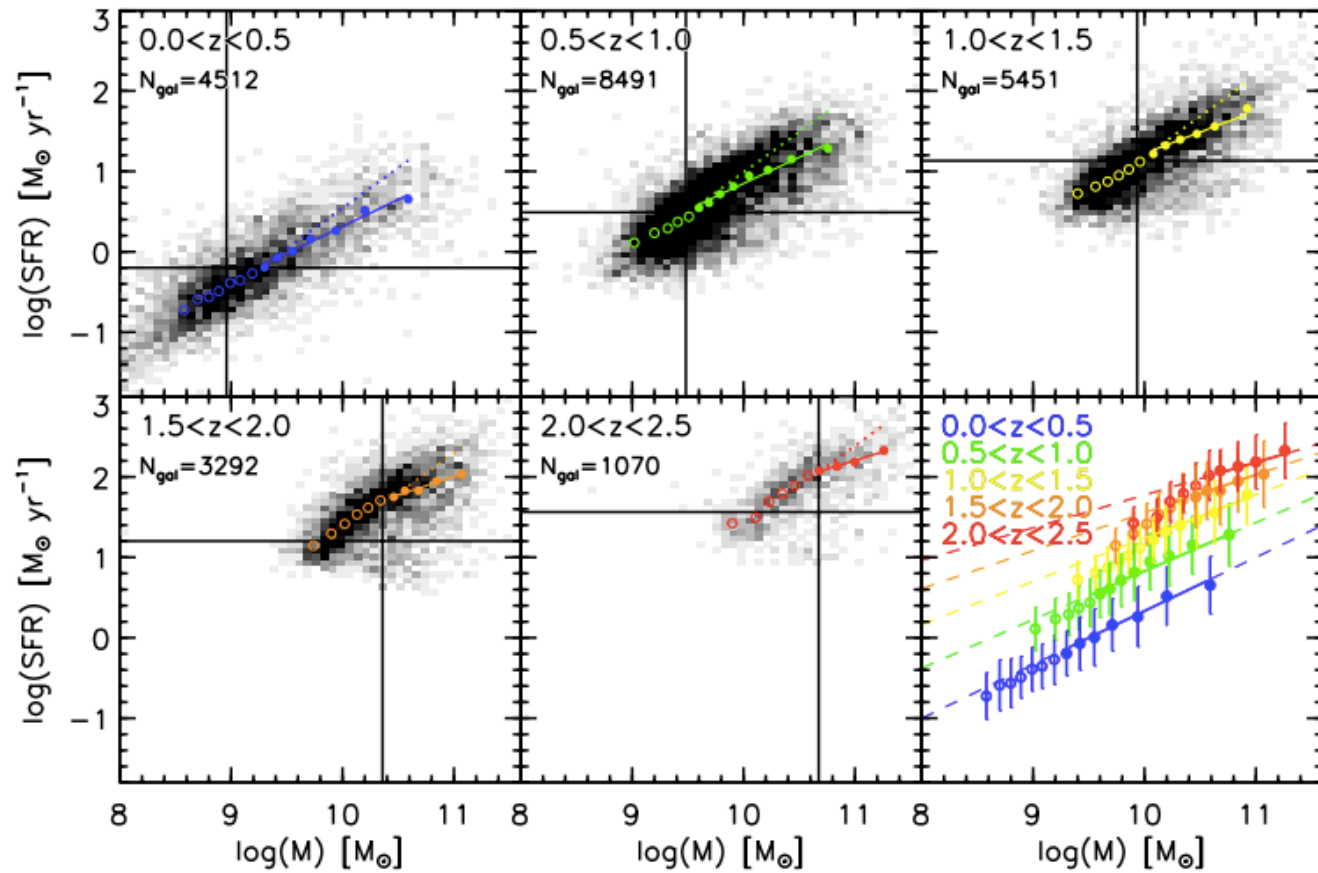
$$\beta(z) = 0.38 + 1.14z - 0.19z^2.$$

The slope of this relation is the specific star formation rate
 $\text{sSFR} = \text{SFR} / M^*$



Star Formation Main Sequence

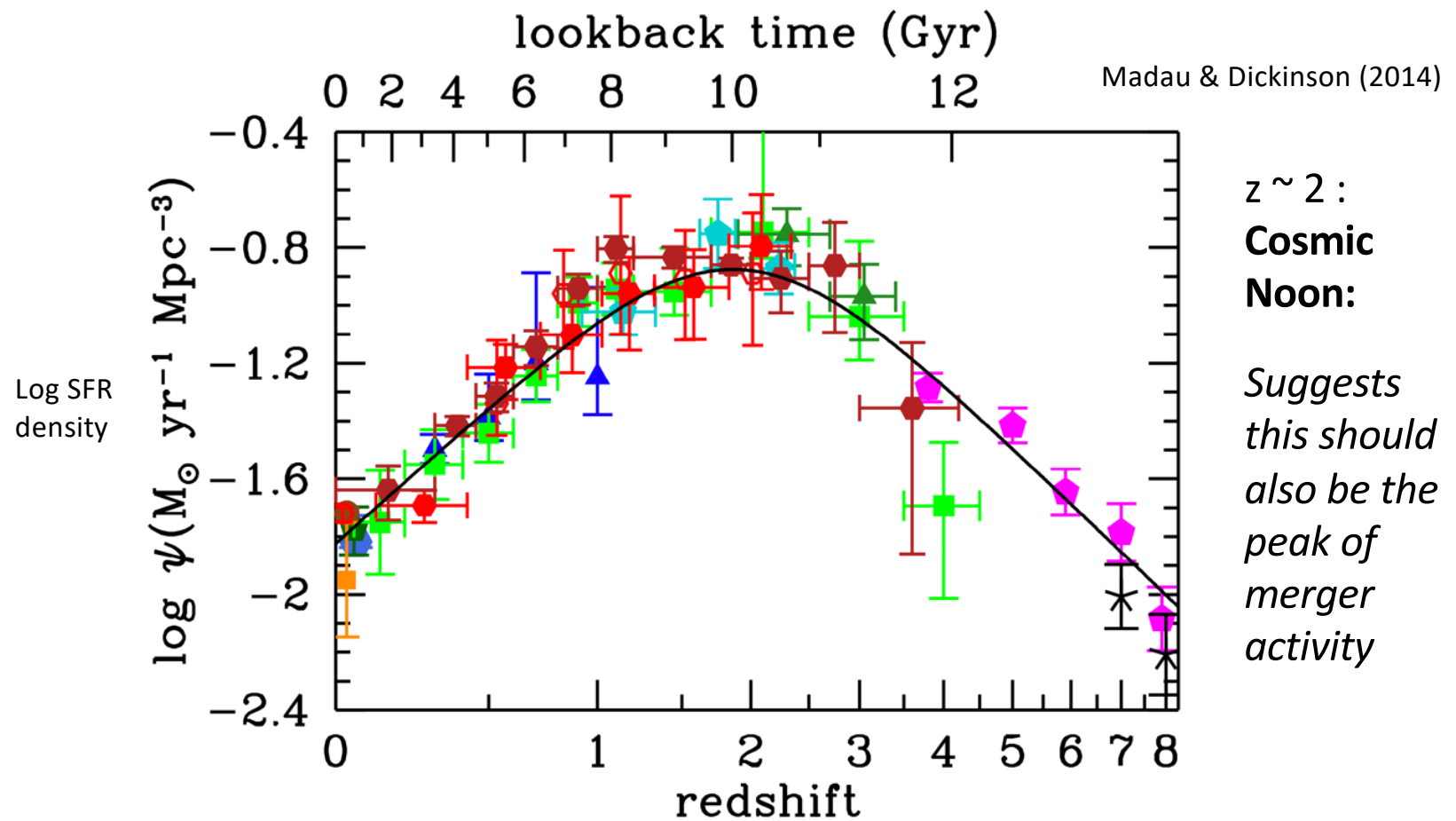
Whitaker+2012



Cosmic downsizing:
Total star formation is dominated by lower mass galaxies over time

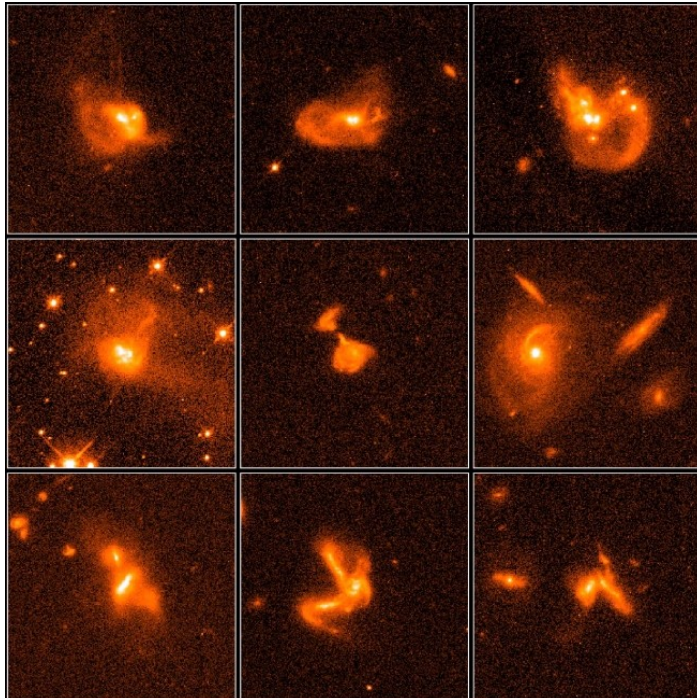
Figure 1. SFR mass sequence for star-forming galaxies has a nonlinear slope at $0 < z < 2.5$ (dotted line is linear). The running medians and scatter are color-coded by redshift, with a power law fit above the mass and SFR completeness limits (solid lines in bottom-right panel). ³²

$z \sim 1 - 3$: Peak Epoch of Cosmic Star Formation Activity

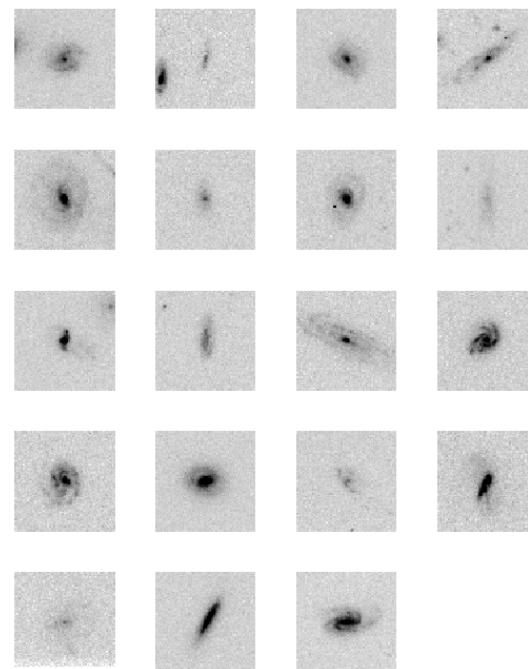


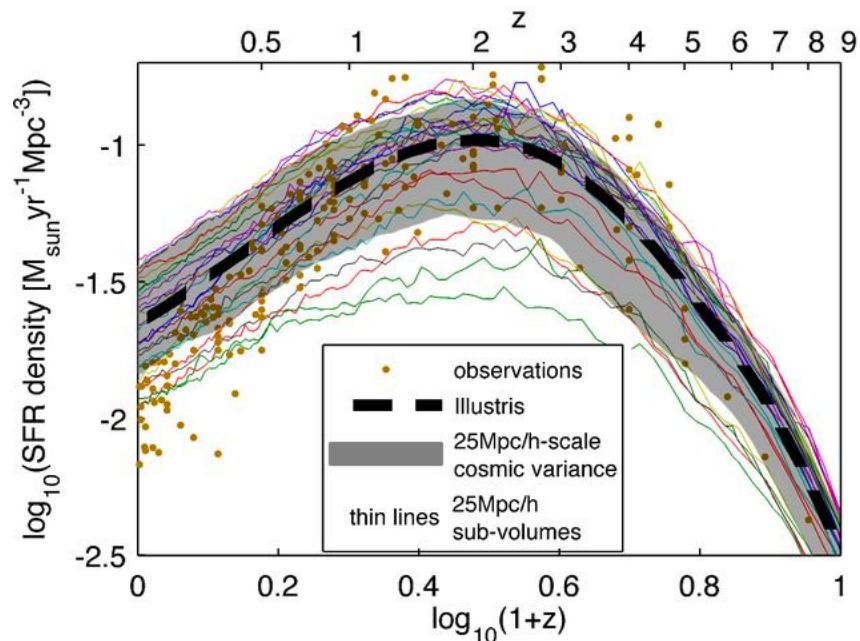
Galaxy Evolution

Galaxies at $z > 2$ are multiple with evidence of merging



Assembly of large Galaxies was evidently completed at $z < 1$

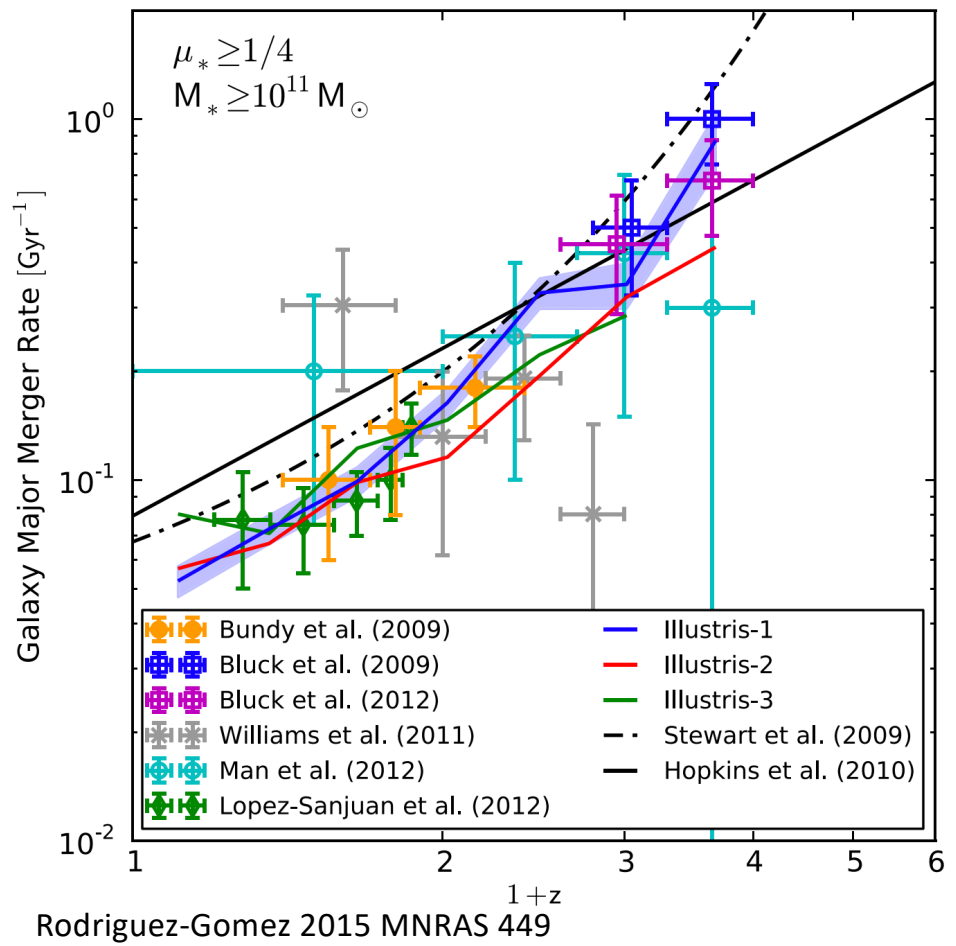




(a) Cosmic SFR density, 35.5 Mpc cosmic variance

Genel+2014. MNRAS 445

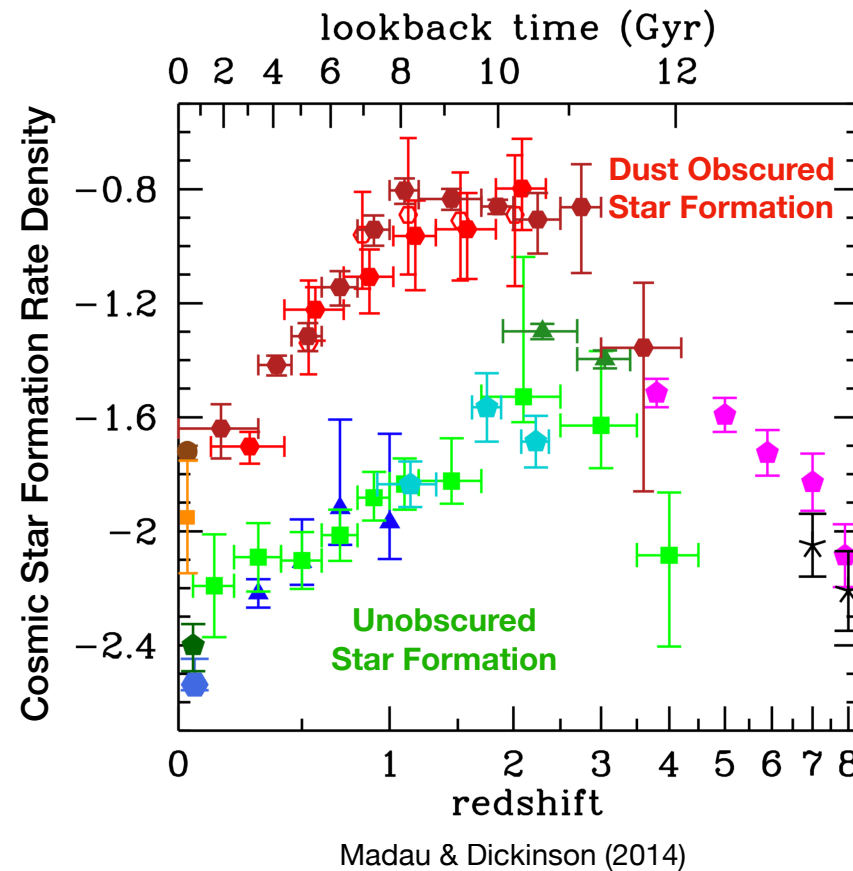
Illustris



Rodriguez-Gomez 2015 MNRAS 449

Illustris: Merger Rate doesn't peak at z~2

SIGNIFICANT FRACTION OF STAR FORMATION IS DUST OBSCURED AT HIGH REDSHIFTS



Madau & Dickinson (2014)

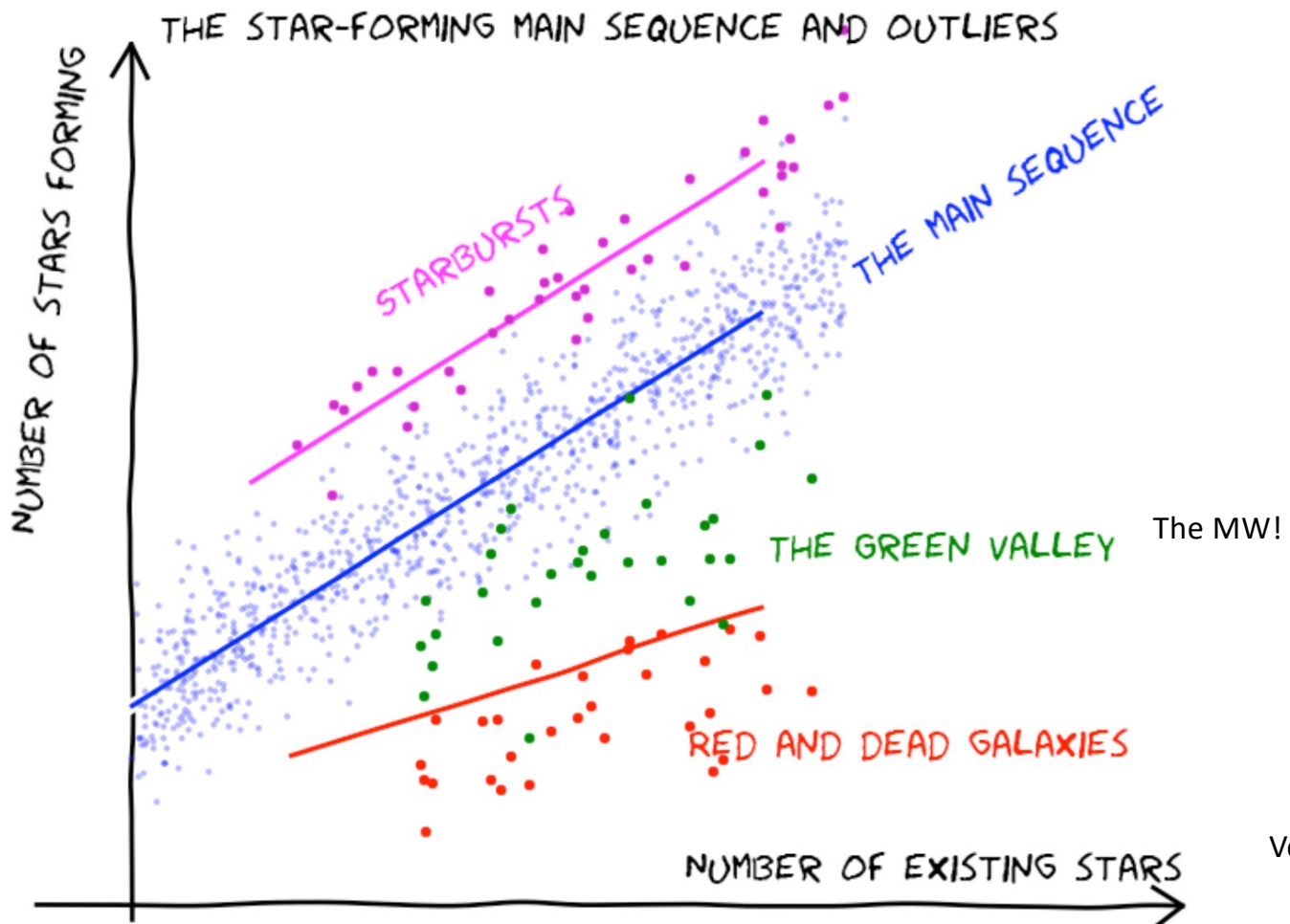


Starburst galaxies

A “starburst” = SFR 3x higher than the average SFR

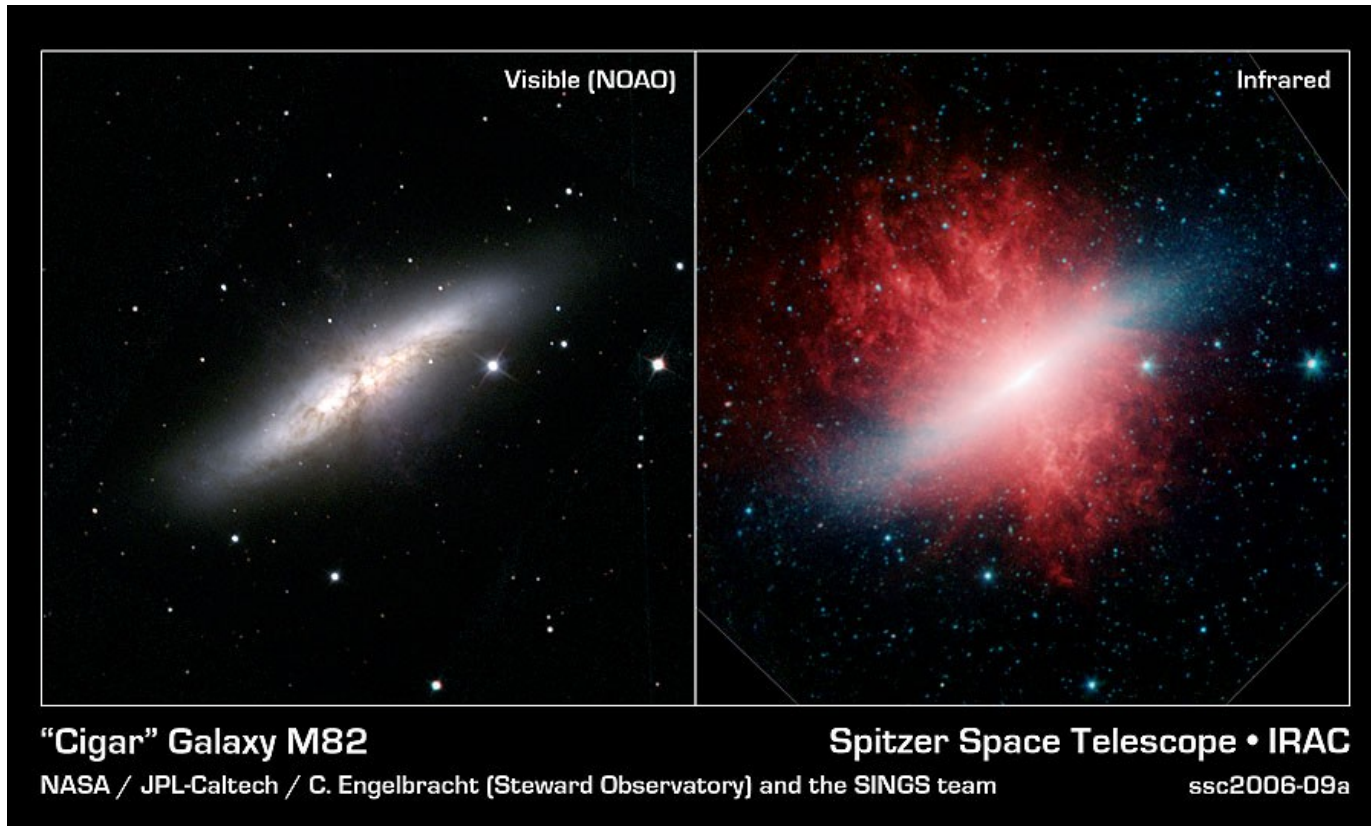
Starburst measured by infrared luminosity 8-1000 μm :
LIRG = Luminous infrared galaxies

Name	$L_{\text{ir}} [L_{\odot}]$	$M(H_2) [M_{\odot}]$	SFR (Msun/year)
normal	10^{10}	10^8	
LIRG	10^{11}	10^9	
ULIRG	10^{12}	10^{10}	
HLIRG	10^{13}	10^{11}	



Veronique Buat

M82 – a nearby starburst



M82 – a nearby starburst

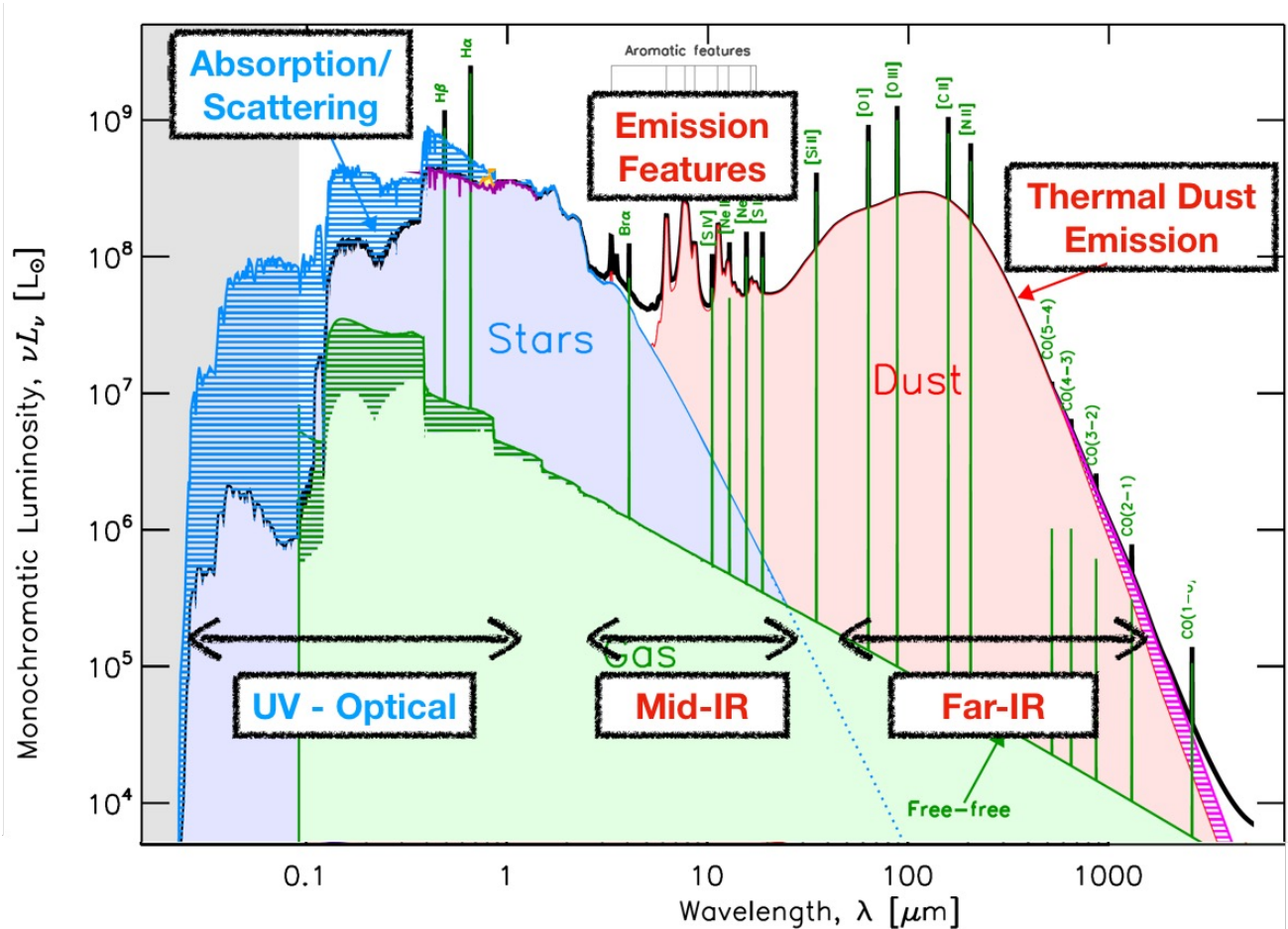


Red: Spitzer IR, Blue: Chandra X-ray

SED of an LIRG

Dust modifies our view of galaxies

Absorbs and scatters UV and optical
Re-emits in IR



Slide: Irene Shivaei

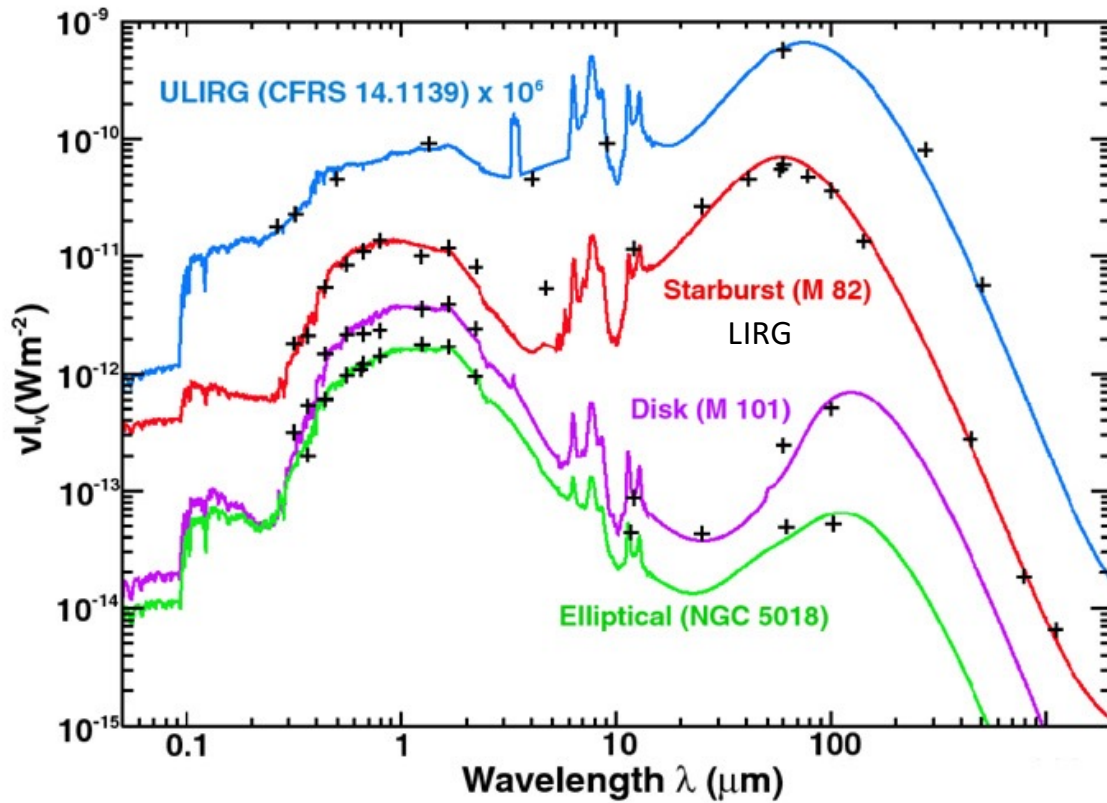
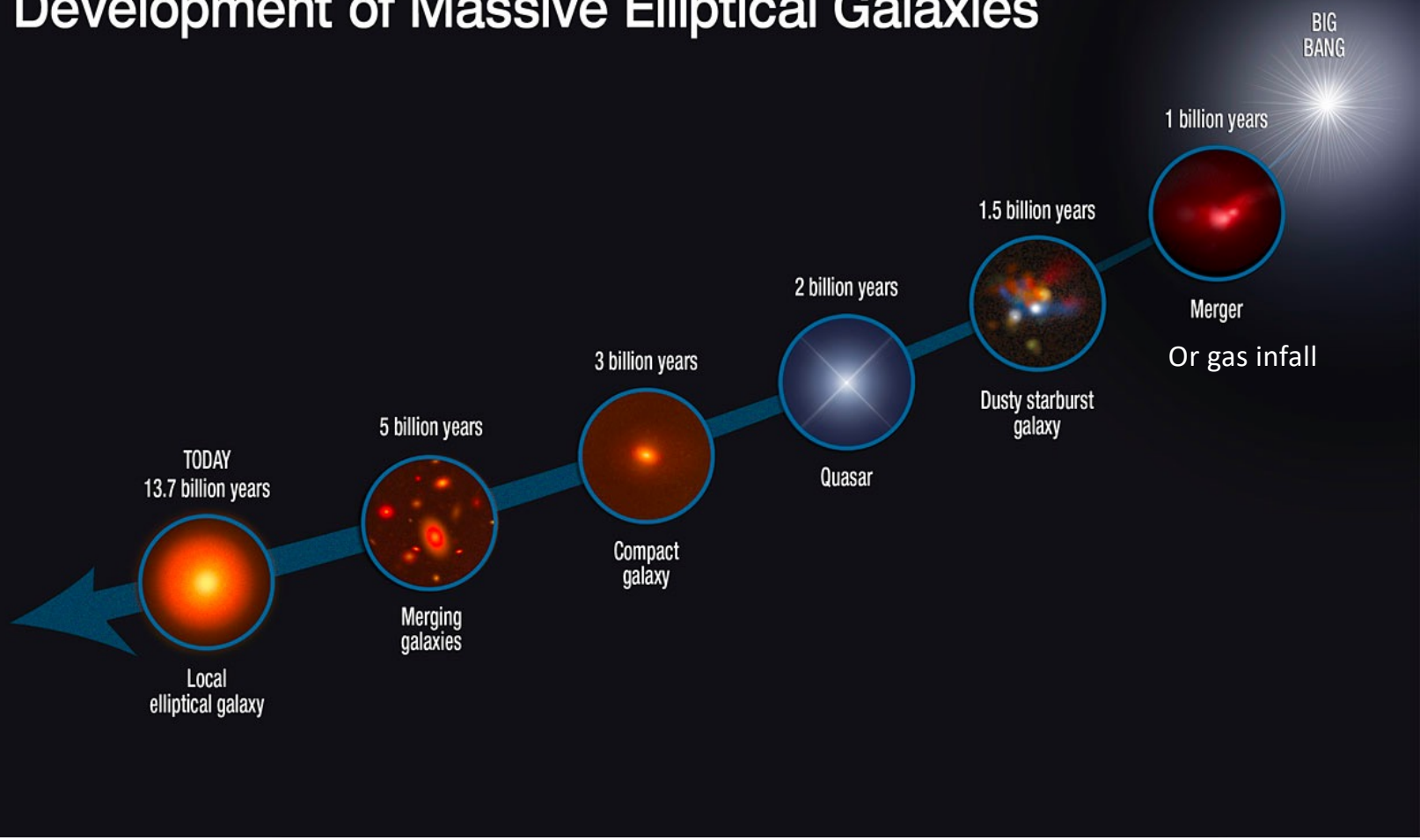


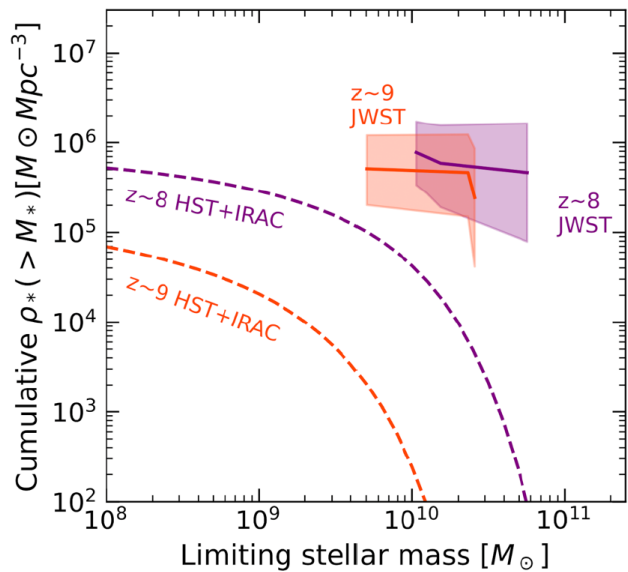
Fig 7.7 (P. Chanial, G. Lagache) 'Galaxies in the Universe' Sparke/Gallagher CUP 2007

Normal elliptical and disk galaxies are brightest in the visible and near-infrared, at wavelengths less than 2 micron. Most dust grains are cooler than 30 K, and their emission peaks beyond 100 micron. In the starburst (LIRG) M82 and the ultra luminous infrared galaxy (ULIRG), dust intercepts far more of the light, and it is hotter, radiating mainly at less than 100 micron.

Development of Massive Elliptical Galaxies



JWST



Article | Published: 22 February 2023

A population of red candidate massive galaxies ~600 Myr after the Big Bang

Ivo Labb  , Pieter van Dokkum, Erica Nelson, Rachel Bezanson, Katherine A. Suess, Joel Leja, Gabriel Brammer, Katherine Whitaker, Elijah Mathews, Mauro Stefanon & Bingjie Wang

Nature **616**, 266–269 (2023) | [Cite this article](#)

Labb  +2023. *Nature* 616

Figure 4: **Cumulative stellar mass density, if the fiducial masses of the JWST-selected red galaxies are confirmed.** The solid symbols show the total mass density in two redshift bins, $7 < z < 8.5$ and $8.5 < z < 10$, based on the three most massive galaxies in each bin. Uncertainties reflect Poisson statistics and cosmic variance. The dashed lines are derived from Schechter fits to UV-selected samples.³ The JWST-selected galaxies would greatly exceed the mass densities of massive galaxies that were expected at these redshifts based on previous studies. This indicates that these studies were highly incomplete or that the fiducial masses are overestimated by a large factor.

Submillimeter Galaxies (SMG)

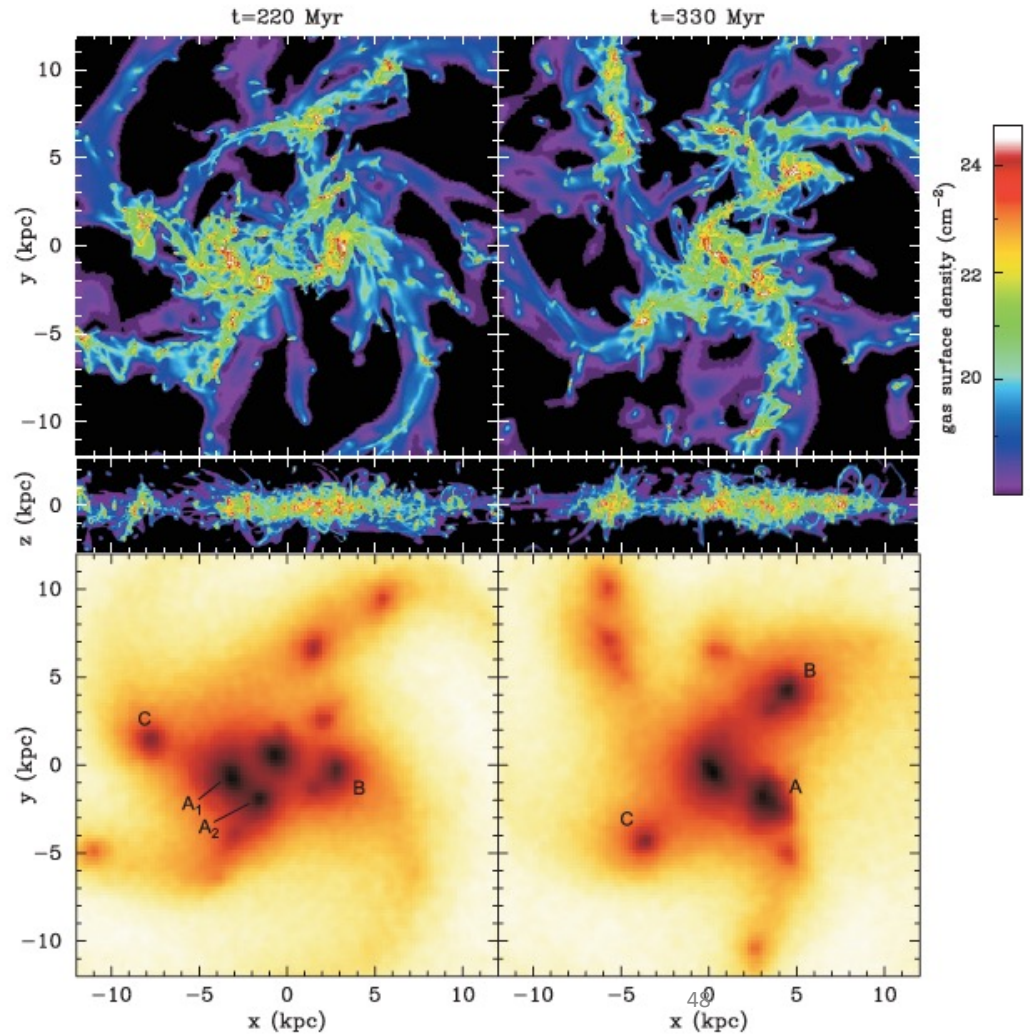
- A class of very bright ULIRGs observed at high z
- Defined as SMG if detected in the sub-mm: 850 μ m flux density > 3-5 mJy (Blain+2002, Smail+1997)
- Required $L_{IR} > 10^{12}$ Lsun ~ ULIRG
- $L_{bol} \sim 10^{12-13}$ Lsun ; Kovacs+2006
- Massive H₂ reservoirs (10^{10-11} Msun; Tacconi+2008)
- Believed to be driven by dust-enshrouded starbursts at $z \sim 1-4$

Origin of Starbursts: Gravitational Instabilities?

Toomre Q < 1

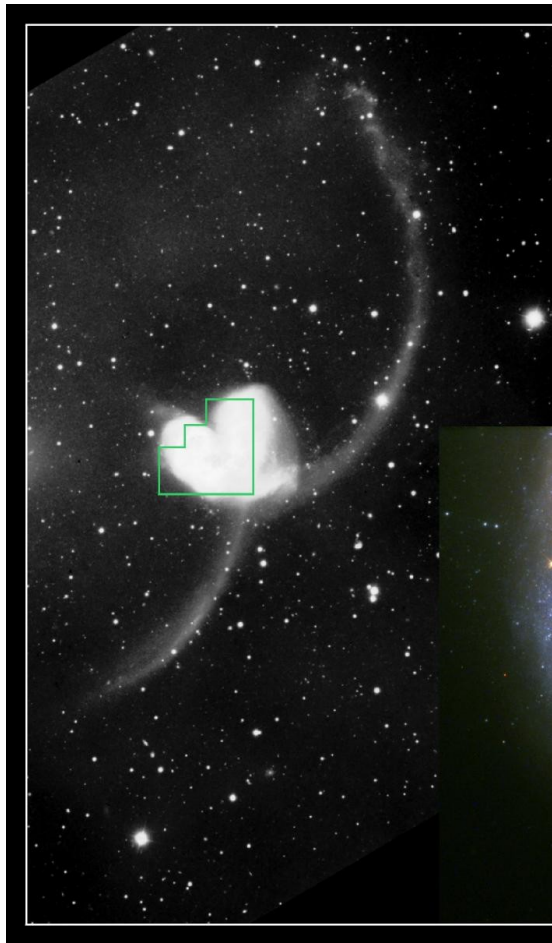
$$Q = \frac{\Omega\sigma}{\pi G \Sigma}$$

Bournaud (2011), Dekel (2009)



Starbursts: Merger Connection?

Antennae – a massive starburst



Optical image

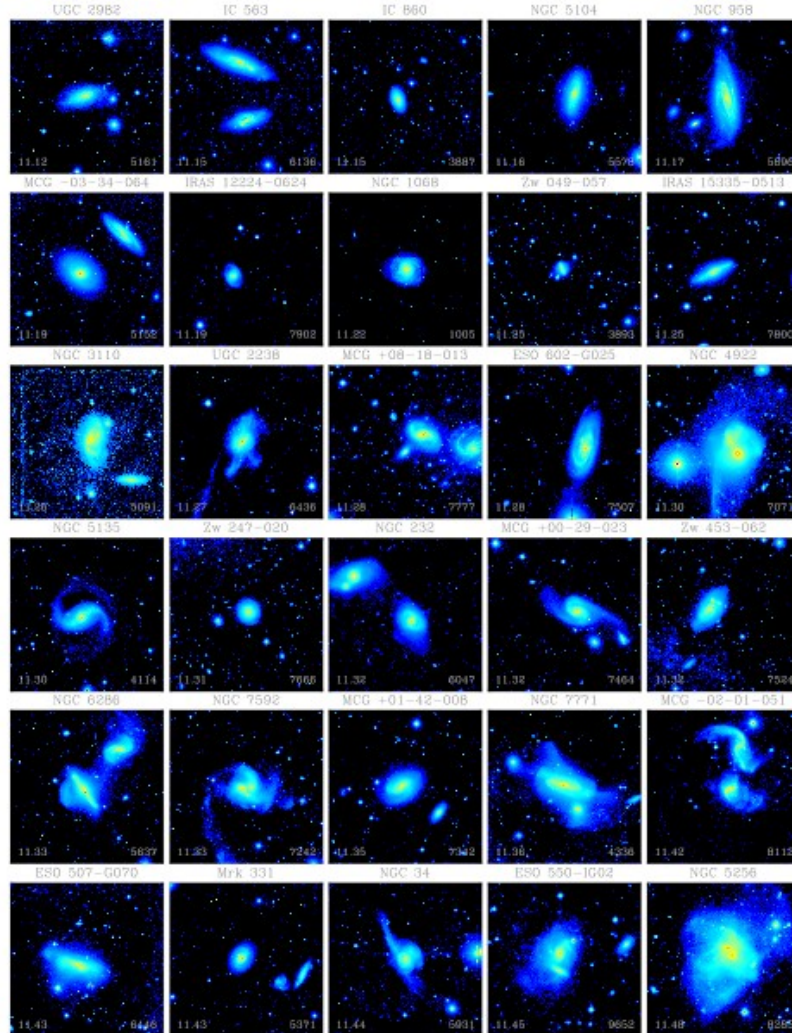


Mid-Infrared

Optical Images of LIRGs

IRAS selected:
 $\log L_{\text{IR}} = 11 - 12$

- Confirm merger origin of most star bursts



Ishida, ApJL (2003)

Brightest: Combination of all things ...

- Narayanan+2015 (Gizmo, cosmological zoom)
- Sub-mm luminous phase is associated with significant mass buildup in early Universe proto-clusters – composed of numerous unresolved components
- SMGs would trace major overdensities

“Submillimeter-emission region probed in surveys typically encompasses a central galaxy in a massive halo that is undergoing a protracted bombardment phase by numerous sub-halos” Flux is dominated by central, but 30% from other galaxies in region.

